

PHYSICAL REVIEW C

NUCLEAR PHYSICS

THIRD SERIES, VOL. 5, No. 1

JANUARY 1972

Neutron Total Cross Sections of the Light Elements in the Energy Range 24–60 MeV*

M. Auman, F. P. Brady, J. A. Jungerman, W. J. Knox, M. R. McGie,† and T. C. Montgomery
Crocker Nuclear Laboratory, University of California, Davis, California 95616
(Received 17 September 1971)

The neutron total cross sections of natural Be, C, N, O, Mg, Al, and Si have been measured at a number of energies between 24 and 60 MeV. The over-all precision is better than 1% and the energies have been determined to 100 keV. Smooth variations of the cross sections with energy are found.

I. INTRODUCTION

Neutron total cross sections are useful in optical-model analyses and for determining the imaginary part of the scattering amplitude at 0° . Peterson¹ has interpreted the energy variation of total cross section in terms of the nuclear Ramsauer effect.

In this experiment a nearly monoenergetic neutron beam has been used to measure total neutron cross sections of natural Be, C, N, O, Mg, Al, and Si at a number of neutron energies in the 24–60-MeV region. The over-all precision of the cross-section determination is typically 0.15 to 0.5%, and that of the energy determination better than 100 keV.

Previous measurements of the total cross section (σ_T) to a precision of a few percent have been made for some of these nuclei within this energy range at Harwell^{2,3} and Livermore.^{4,5} Concurrent with this work, measurements are being made in Manitoba.⁶

II. EXPERIMENTAL TECHNIQUE

The experimental arrangement is shown in Fig. 1. A 5–10- μ A proton beam from the isochronous cyclotron of Crocker Nuclear Laboratory⁷ strikes

a metallic ${}^7\text{Li}$ target, and neutrons from the reaction ${}^7\text{Li}(p, n){}^7\text{Be}$ are collimated at 0° by the 1.55-m-long steel collimator. A well-defined beam of size 15×15 mm and of intensity $2 \times 10^5/\text{cm}^2$ sec is formed. Target samples of 25.4-mm diameter were optically aligned to 0.3 mm on the beam line.

The collimated beam passed in sequence through a neutron detector telescope, the sample position, and, in series, a second and third detector telescope. Each telescope contained a veto scintillator, a CH_2 converter, and two more thin (1 mm) scintillators separated by a copper absorber. The discriminator thresholds of S1 and S2 were set in the middle of the coincidence count-rate plateaus due to recoil protons from the CH_2 . The telescopes are insensitive to γ rays and electrons. Their neutron-detection efficiency is about 1%.

Roughly 60% of the neutrons produced in the reaction ${}^7\text{Li}(p, n){}^7\text{Be}$ fall within a well-defined high-energy peak about 2 MeV wide⁷ corresponding to transitions principally to the ground state of ${}^7\text{Be}$. The remaining neutrons are spread over a broad, lower-energy tail. Only neutrons in the narrow, high-energy peak, selected by time of flight, were used in the transmission measurements. The copper absorber in each detector telescope eliminated recoil protons due to lower-energy neutrons

from earlier beam bursts. Thus the neutrons utilized for the measurements were selected to be monochromatic with a full width at half maximum of 2 MeV. The mean energy of the beam was determined to better than 100 keV by a time-of-flight measurement.⁸

The samples were cylinders 63 mm to 127 mm long, and most were machined from high-purity material (99.9%) which had been quantitatively analyzed. In addition, the samples were x-rayed for voids. Densities and lengths of samples were accurately determined by micrometer measurements and weighing. Cross-section measurements were made with samples of Be, C, CH₂, CH₂N₂ (melamine), Mg, SiO₂, Al, and Al₂O₃. The latter two gave the total cross section for O and Al; CH₂N₂ gave the N cross section, and SiO₂ gave the Si cross section. A copper cylinder 45.7 cm long was used in the sample position during background runs.

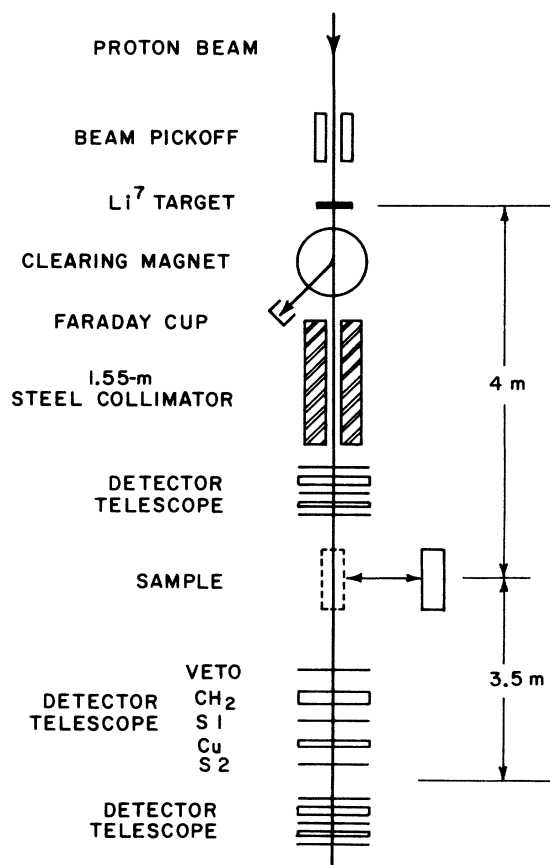


FIG. 1. Experimental arrangement for total-cross-section measurements. The nearly monochromatic peak of the neutron beam was monitored before and after the sample. The latter was cycled automatically in and out of the beam.

The counting rate of the detector telescope preceding the sample monitored the incident beam intensity (I), while the counts from the telescopes following the sample were combined to measure the transmitted intensity (T). The I and T counting rates were printed out automatically as samples were cycled in and out of the beam about every 5 min. The transmission ratio R was computed as T/I for the sample out of the beam divided by T/I for the sample in the beam. The uncorrected cross section for the sample is then given by $\sigma_T = K \ln R$, where K is the inverse of the number of atoms or molecules per unit area presented by the sample to the beam and is determined from measurements of the sample sizes and weights.

III. ANALYSIS

The data analysis consisted mainly of applying corrections and estimating uncertainties. Corrections were made for background, air displacement, dead time, finite solid angle, and hardening. The total of all corrections was typically one half of one percent. Details of the corrections are given below followed by estimates of uncertainty in the total cross section.

A. Background

Background was measured at each energy by placing a 2.54-cm-diam, 45.7-cm-long copper bar at the sample position. Transmission of neutrons through the copper bar was negligible. The correction due to background counts is given by

$$\Delta\sigma_T = -K \left(\frac{B}{N_o} - \frac{B}{N_i} \right),$$

where B is the normalized background counting rate, and N_i and N_o are the normalized counting rates with the sample in and out, respectively. This equation includes background counts due to neutrons scattered by the sample and rescattered by the surroundings into the detector, and counts due to neutrons aside from those in the transmitted beam which enter the detector without scattering in the sample. The ratio B/N_i was typically 10^{-4} . This correction was of the order of 0.1%.

B. Air Displacement

The correction to compensate for displacement of air by the sample was

$$\Delta\sigma_T = nLK\sigma_a,$$

where n is the number of air nuclei per unit volume, L is the length of the sample, and σ_a is the average total cross section for air nuclei. This correction was of the order of 0.1% also.

TABLE I. Corrections applied at 46.18 MeV.

Target	Uncorrected σ_T	Corrections applied to uncorrected σ_T in mb						Corrected σ_T (mb)
		Background	Air displacement	Dead time	Hardening	Finite solid angle	Impurities	
Be	805.38	0.85	0.49	1.85	0.0	0.15	1.25	809.97
C	1008.46	1.45	0.68	1.90	0.02	0.22	0.0	1012.73
N	1172.64	1.16	0.77	3.27	0.25	0.30	0.0	1178.39
O	1285.80	2.47	0.43	2.16	0.09	0.35	-4.07	1287.23
Mg	1656.63	1.56	1.34	3.88	0.07	0.56	0.70	1664.74
Al	1749.95	1.48	1.00	4.71	0.16	0.62	6.11	1764.03
Si	1833.03	0.50	1.93	5.61	-0.16	0.68	9.11	1850.72

C. Dead Time

Counts from the transmission monitor are inevitably lost because of the dead time of the time-to-amplitude converter (TAC). The correction to the cross section for this effect is

$$\Delta\sigma_T = KN_o \Upsilon(1 - R^{-1}),$$

where N_o is the counting rate with sample out, and Υ is the dead time of the TAC (about 4.6 μ sec). The order of magnitude of the dead-time correction was 0.1%.

D. Inscattering and Finite Solid Angle of Detector

There are two ways a neutron which is scattered out of the beam can be detected by the transmission monitor: (1) The neutron can be scattered by additional encounters in the sample so that it is detected by the monitor; and (2) the neutron can be scattered at a sufficiently small angle so that it remains in the solid angle of acceptance of the transmission detector. This latter effect, when analyzed for the geometry of this experiment, results in the correction

$$\Delta\sigma_T = \frac{d\sigma}{d\Omega}(0^\circ)\Delta\Omega,$$

where $(d\sigma/d\Omega)(0^\circ)$ is the differential cross section for forward elastic scattering, and $\Delta\Omega$ is the solid angle subtended by the transmission detector at the sample position. The differential cross section was taken to be Wick's limit $(k\sigma_T/4\pi)^2$, where k is the wave number of the neutron. This correction amounted to a few hundredths of a percent. The multiple-scattering effect can be estimated to be about one tenth of the finite-solid-angle effect and was therefore neglected.

E. Hardening

Significant errors are introduced into the measurements as a result of energy spread in the neutron beam whenever: (1) There is a sufficiently rapid variation in the total cross section with energy, or (2) the second derivative is sufficiently large. A large first derivative causes the average neutron energy to shift significantly as the beam progresses through the sample. A large second derivative causes the cross section averaged over the neutron-energy peak to be different from the cross section at the mean energy.

The energy spread of the neutrons in the full-energy peak is due mostly to energy losses of the incident protons in the Li target prior to neutron production. This energy loss ranges from zero to

TABLE II. Total cross sections (in mb) with over-all uncertainties.

Target	Energy (MeV)							
	24.63	29.25	36.34	39.56	46.18	49.06	54.37	58.90
Be	971.3 \pm 2.3	...	810.0 \pm 1.7	762.2 \pm 1.7	696.6 \pm 1.8	641.6 \pm 1.6
C	1389.6 \pm 1.7	1311.2 \pm 1.7	1179.3 \pm 1.4	1130.7 \pm 1.2	1012.7 \pm 1.4	961.8 \pm 1.0	883.3 \pm 1.1	821.8 \pm 1.5
N	1333.0 \pm 7.8	...	1178.4 \pm 5.8	1109.6 \pm 5.2	1016.8 \pm 4.2	951.0 \pm 5.6
O	...	1578.2 \pm 8.3	1460.6 \pm 8.1	1412.4 \pm 6.6	1287.2 \pm 6.5	1228.4 \pm 5.4	1149.0 \pm 6.1	1066.4 \pm 5.4
Mg	1789.1 \pm 7.4	...	1664.7 \pm 7.7	1616.8 \pm 5.3	1534.5 \pm 6.3	1448.0 \pm 4.6
Al	...	1885.8 \pm 8.2	1871.3 \pm 8.9	1854.3 \pm 6.8	1764.0 \pm 5.9	1712.0 \pm 5.3	1619.2 \pm 6.1	1539.7 \pm 5.4
Si	...	1960 \pm 25	1971 \pm 20	1937 \pm 16	1851 \pm 16	1800 \pm 14	1696 \pm 15	1621 \pm 13

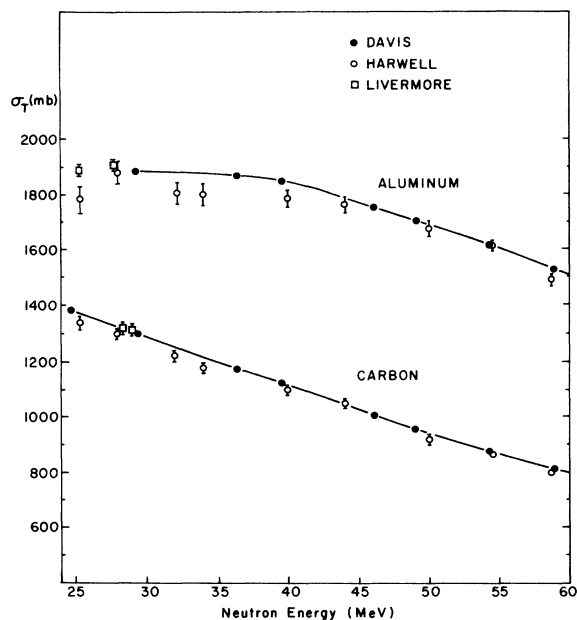


FIG. 2. Total cross sections for aluminum and carbon samples are shown. Errors in the Davis data are too small to be displayed in the figure, but are tabulated in Table II. Data from Harwell (Ref. 3) and Livermore (Ref. 5) are also shown for comparison.

some maximum value which depends on target thickness and proton energy, with all intermediate values equally probable. Thus the neutron-energy distribution is nearly flat with a width determined by the beam energy and the Li target thickness.

If we assume a flat neutron-energy distribution of half-width E , we obtain for the correction

$$\Delta\sigma_T = \frac{E^2}{6} \left[\frac{1}{K} \left(\frac{d\sigma_T}{dE} \right)^2 - \frac{d^2\sigma_T}{dE^2} \right].$$

The result is a small correction of the order of a few hundredths of a percent.

F. Impurities

Impurities in all of the samples except carbon and melamine (CH_2N_2) ranged up to 1%. The melamine sample was tested and found to have no detectable impurities. The carbon samples were spectroscopic-grade carbon. Corrections were calculated for the other samples from measurements or estimates of the total cross sections of

these impurities. Where estimates were made they were made by using the $\sigma \propto A^{2/3}$ relationship and applying it to measured cross sections of elements whose atomic weights were close to the impurity atomic weight. The corrections were less than 0.2% for all but one case, which was approximately 0.4%; they did not require precise σ_T values for the impurities.

G. Uncertainties

The principal uncertainty attributed to each cross section is due to counting statistics. In addition 20% of the background correction, 30% of the dead-time correction, and 50% of the correction for impurities were folded in. An additional uncertainty is associated with the energy measurement, which is typically uncertain by about 100 keV in most cases. Since the variation of total cross section with energy is typically only 0.15% per 100 keV, the energy uncertainties have not been translated into total-cross-section uncertainties. In Table I corrections are shown for the one energy, 46.18 MeV.

IV. RESULTS

The corrected total-cross-section values are given in Table II. No previous measurements have been made for Be, N, O, Mg, or Si in this energy range except near 29 MeV by Peterson, Bratenahl, and Stoering,⁵ and the values for all seven of the elements at this energy are in good agreement. Bowen *et al.*³ have measured the total cross section of C and Al over the energy range of this work, and although agreement is generally within the uncertainty limits, the present results are consistently slightly larger than those of Bowen *et al.* for both elements. Figure 2 displays the results for aluminum and carbon.

The authors thank Dr. Juan Romero and Robert Walraven for assistance in taking data, Walter Kemmler and Louis Vogt for precision machining of the samples, and the Crocker Nuclear Laboratory cyclotron crew for the good beams. We are grateful to Lawrence Radiation Laboratory, Livermore, and Dr. J. P. Peterson for loaning us many of the samples, and to the Davis Trace Element Analysis Group for analyzing some of the samples.

*Work supported in part by the U. S. Atomic Energy Commission.

†Present address: Chico State College, Chico, California.

¹J. M. Peterson, Phys. Rev. **125**, 955 (1962).

²A. E. Taylor and E. Wood, Phil. Mag. **44**, 95 (1952).

³P. H. Bowen, J. P. Scanlon, G. H. Stafford, J. J. Thresher, and P. E. Hudgson, Nucl. Phys. **22**, 640 (1961).

⁴A. Bratenahl, J. M. Peterson, and J. P. Stoering, Phys. Rev. **110**, 927 (1958).

⁵J. M. Peterson, A. Bratenahl, and J. P. Stoering, *Phys. Rev.* **120**, 521 (1960).

⁶I. Bubbe, private communication.

⁷J. A. Jungerman and F. P. Brady, *Nucl. Instr. Methods*

89, 167 (1970).

⁸F. P. Brady, W. J. Knox, and S. W. Johnsen, *Nucl. Instr. Methods* **89**, 309 (1970).

PHYSICAL REVIEW C

VOLUME 5, NUMBER 1

JANUARY 1972

Reaction $^{20}\text{Ne}(^3\text{He},\alpha)^{19}\text{Ne}$ at 18 MeV*

D. S. Haynes,† K. W. Kemper, and N. R. Fletcher

Department of Physics, The Florida State University, Tallahassee, Florida 32306

(Received 14 July 1971)

Excitation energies of the states in ^{19}Ne are measured via the reaction $^{20}\text{Ne}(^3\text{He},\alpha)^{19}\text{Ne}$ up to an excitation of ~ 10.6 MeV. Angular distributions for several states are measured and analyzed by use of the conventional distorted-wave Born approximation. Relative spectroscopic factors are extracted and compared with the predictions of the spectroscopic-factor sum rule. The analysis fails to confirm an assignment of $j = \frac{3}{2}$ for the excited states at 6.01 and 6.74 MeV.

I. INTRODUCTION

Prior to 1969 there was very little experimental information on the energy-level structure of ^{19}Ne although model calculations for the structure of the mass-19 system had been a topic of considerable interest.¹ Early measurements involving the reaction $^{19}\text{F}(p,n)^{19}\text{Ne}$ established the existence of six excited states below 2.8 MeV with some spin and parity assignments.² More recent investigations of the reactions $^{20}\text{Ne}(^3\text{He},\alpha)^{19}\text{Ne}$ and $^{17}\text{O}(^3\text{He},n)^{19}\text{Ne}$ have fixed the spin and parity assignments of these first six states³ and extended the known excitation-energy region to ≤ 5.1 MeV.^{4,5}

Recent work by Gill *et al.*⁶ has accurately established the excitation energies of the first six states and confirmed the spin and parity assignments of Olness and Warburton.³ The measurements by Garrett, Middleton and Fortune (GMF)⁷ of α -particle energies from the reaction $^{20}\text{Ne}(^3\text{He},\alpha)^{19}\text{Ne}$ yield excitation energies in agreement with previous values, and they report several additional levels between 5.1 and 7.1 MeV in excitation.

The present measurement of the reaction $^{20}\text{Ne}(^3\text{He},\alpha)^{19}\text{Ne}$ at $E_{^3\text{He}} \approx 18$ MeV proposes excitation energies for 21 more states in ^{19}Ne between 7.1- and 10.6-MeV excitation, which extends well into the excitation-energy region in which states may be investigated by the $^{16}\text{O} + ^3\text{He}$ resonance reactions.⁸ Excitation energies determined for previously reported levels are generally in quantitative agreement. Some extracted spectroscopic factors differ appreciably from the values of GMF.⁷ The distorted-wave Born-approximation (DWBA)

calculations for a few of the higher excited states do not lead to conclusive orbital angular momentum transfer assignments.

II. CALIBRATION AND ENERGY LEVELS

For accurate energy-level determination it is essential to maximize the statistical accuracy of the spectra, to be able to calculate the energy distribution within a single spectral line for spectrum stripping, and to ensure a stable and accurate calibration. A computer code developed to calculate spectral line shape has been shown to predict accurately the shape and energy width of observed groups in energy spectra.⁹ The use of the code was instrumental in designing a gas target system for maximum count rate and minimum detected energy spread. The gas cell used had a surface-barrier detector placed inside the target gas volume sealed by a beam entrance window of 0.5- μm nickel. Parameters pertinent to energy resolution and those values used in the present experiment have been reported.⁹ Isotopically enriched gas of 99.7% ^{20}Ne was used and all calibration spectra were digitally stabilized.

A. Calibration

For calibration and Q-value analysis, six reaction angles were chosen with nominal values of $\theta = 27.8, 32.8, 37.5, 47.5, 52.5,$ and 57.5° with a possible error of $\pm 0.1^\circ$. Gas pressure was maintained at ~ 50 Torr for the two forward-angle spectra and at ~ 100 Torr for the other four spectra. The spectra for $\theta = 27.8$ and 37.5° are shown in Fig. 1. Centroids and yields of energy groups in the